Physics and Chemistry of the Earth 36 (2011) 1511–1520

Contents lists available at SciVerse ScienceDirect

Physics and Chemistry of the Earth

journal homepage: www.elsevier.com/locate/pce

Dissolved helium distribution in the Oxfordian and Dogger deep aquifers of the Meuse/Haute-Marne area

E. Fourré [a,*], P. Jean-Baptiste [a], A. Dapoigny [a], B. Lavielle [b], T. Smith [b], B. Thomas [b], A. Vinsot [c]

[a] LSCE, UMR 8212, CNRS-CEA-UVSQ/IPSL, 91191 Saclay, France
[b] CNAB, UMR 5084, Université de Bordeaux 1, 33175 Gradignan, France
[c] ANDRA, 92290 Châtenay-Malabry et Centre de Meuse/Haute-Marne, 55290 Bure, France

ARTICLE INFO

Article history:
Received 14 May 2011
Accepted 4 October 2011
Available online 8 October 2011

Keywords:
Helium isotopes
Groundwaters
Residence time
Paris Basin
Dogger
Oxfordian

ABSTRACT

The 140-m-thick, clay-rich Callovo-Oxfordian (COX) layer of the eastern Paris Basin, France, is being considered by the French Nuclear Waste Agency (Andra) as a long-term underground nuclear waste repository. Andra has selected a 250 km^2 area (transposition zone) to be further characterised, especially in view of the confinement properties exhibited by the COX. This study reports the helium concentrations and isotopic ratios of water samples from the aquifers above and below the COX, which are the Oxfordian and Dogger aquifers, respectively. The samples were collected from five drilling sites (2007–2008). Both the Oxfordian and Dogger groundwaters are of meteoric origin and have accumulated radiogenic He with a $^3He/^4He$ ratio of approximately 0.02 Ra. The He concentrations in the groundwaters are two orders of magnitude higher than in the air-saturated water in the Oxfordian and approximately 10 times higher in the Dogger than in the Oxfordian. One borehole was drilled down into the Triassic sediments, allowing a sample to be collected from the Bundsandstein aquifer. Here, the He concentration is of the same order of magnitude as those measured in the Dogger, but the isotopic ratio is slightly higher at 0.04 Ra. However, this ratio is approximately 10 times lower than those measured by Marty et al. (2003) in waters collected closer to the Trias recharge and tagged with mantle-derived He. This lower ratio is most likely due to a significant and rapid slowdown of the circulation in this aquifer, allowing substantial radiogenic He accumulation. A key conclusion of this study concerns the lateral non-homogeneity of the studied area: He concentrations are higher in the northern part of the transposition zone. This observation can be explained by a longer residence time of the waters and/or a higher input of He from the basement. A simplified 2D model of He transport shows that the second hypothesis alone does not allow fitting of the data, thus implying more stagnant water in this area. The indicative residence times derived from this coarse model are 0.3–0.5 Myr (Oxfordian) and 0.5–0.6 Myr (Dogger) for the borehole located in the centre of the investigated zone; for the northernmost borehole, they reach 0.8–1.4 Myr for the Oxfordian and 1.5 Myr for the Dogger.

1. Introduction

Noble gases are useful for studying deep aquifers because they are natural inert tracers that are transported without chemical reaction with the host-rocks. Helium in groundwaters is derived from three sources with distinct isotopic signatures, allowing fluid origin and transport to be traced (Ballentine et al., 2002): (1) the atmosphere, with an isotopic ratio of $^3He/^4He = Ra = 1.384 \times 10^{-6}$ (Clarke et al., 1976); (2) the crust, with $^3He/^4He$ ratios in the range of 10^{-8} and below (radiogenic and, to a lesser extent, nucleogenic He); and (3) the mantle, with $^3He/^4He$ ratios of 8 Ra for the upper mantle and up to approximately 30 Ra at hotspots (primordial origin). Dissolved helium, in particular, is a useful tool for the estimation of residence times of ancient groundwaters (Kipfer et al., 2002). The helium content of groundwater basically depends on two parameters: (1) the helium release rate in the subsurface due to the alpha-decay of U/Th series in aquifer rocks and the underlying basement as well as possible fluxes from the mantle and (2) the residence time of water (i.e., its transit time from the recharge area to the study site). Helium accumulation results in deep groundwater helium concentrations (Ballentine et al., 2002) that can reach up to 3–4 orders of magnitude above ASW (air saturated water). Therefore, provided that the helium fluxes entering and leaving the aquifer can be reasonably estimated, the quantification of the He accumulation rate is a suitable geochronometer for dating groundwaters in deep aquifers.

Here, we report the results of a study conducted on groundwater from the Oxfordian and Dogger deep aquifers in the eastern Paris Basin, France. The Paris Basin (Mégnien, 1980) forms an intracratonic

* Corresponding author. Tel.: +33 1 69 08 41 72; fax: +33 1 69 08 77 16.
E-mail address: elise.fourre@lsce.ipsl.fr (E. Fourré).

1474-7065/$ - see front matter © 2011 Elsevier Ltd. All rights reserved.
doi:10.1016/j.pce.2011.10.006

depression with a diameter of approximately 700 km. The depression was developed by thinning of the underlying crust. The Paris Basin is surrounded by four Hercynian formations: the Massif Central to the south, the Massif Armoricain to the west, and the Vosges and Ardennes to the east and northeast, respectively. To the north and northwest, the basin extends under the English Channel to the London Basin (Fig. 1). Sediments have been deposited since the Triassic in a shallow marine environment over the course of a series of transgressions and regressions, leading to a thick accumulation (up to 3000 m at its centre) of alternating deposits of permeable layers dominated by limestones and sandstones and impervious layers dominated by marls and clays (Fig. 2). One of these aquitards, the clay-rich Callovo-Oxfordian (COX), is of particular interest because it is being considered as a long-term underground nuclear waste depository by the French Nuclear Waste Agency (Andra). In the eastern part of the Paris Basin, Andra has selected an area in the Meuse/Haute-Marne region (east of the basin) that is delimited by the Marne fault to the west and the Gondrecourt faults to the east. This area is also situated far from known seismicity zones (Fig. 3). At this location, within a 1-km-thick sedimentary sequence (Fig. 2), the COX is approximately 140 m thick and is sandwiched by two thick (approximately 300 m) limestone aquifers, the Oxfordian at the top and the Dogger at the bottom.

In the study area, both of these aquifers are fed by meteoric waters infiltrating along the eastern and southeastern outcrops of the Paris Basin, located several tens of kilometres from the drilling sites (Matray et al., 1994; Buschaert et al., 2007; Linard et al., 2010). The general groundwater flow tends towards the north and northwest. Permeabilities in the Oxfordian and Dogger formations are low (10^{-9}–10^{-11} m/s). The porosities are heterogeneous, as determined from the porosity logs (Andra 2009a), with water content varying, for instance, from 1–2% to 16% in weight for the Oxfordian formation. Therefore, single productive levels cannot be followed throughout the studied area because they differ in thickness and relative depth from one borehole to the other.

Six sites (named A–F) have been selected by Andra to further characterise a 250 km^2 zone around the Underground Research Laboratory (URL). Boreholes (one for each studied formation) were drilled in 2007–2008 (Fig. 3). The southeastern part of this zone is an area of secondary faults between the Gondrecourt Fault and the Marne Fault where the microfractures of the limestone formations are more developed than for the other drilling sites. In this area, called the "diffuse fractured zone" by Andra (see Fig. 3), the salinity measurements are not coherent with the piezometric map (Andra 2005), and the hydrology is not yet well understood (transmissive fractures are suspected); hence, further studies are needed in this area.

This paper focuses on the helium isotopic composition of groundwater samples from the Oxfordian and the Dogger to gain better insights into the hydrology of these limestone formations above and below the COX in this area.

2. Sampling and methods

Boreholes penetrating the Oxfordian and Dogger formations were drilled at sites A–C, E and F with a downhole hammer (Fig. 3). Sites E and F are located in the diffuse fractured zone. Site C was selected to be drilled further down into the basal Trias conglomerate; only one sample of brackish-type groundwater could be recovered from this deep drilling (conductivity of 166 mS/cm).

For the Oxfordian waters, the boreholes were drilled over the entire thickness of the Oxfordian limestone. For the Dogger waters, the boreholes were drilled down to approximately 100 m below the top of the formation. Each borehole was cased down to the top of the targeted formation.

For both the Oxfordian and Dogger limestones, the formations are highly heterogeneous, as previously noted, with a few discrete water venues (Table 1). For some major venues, the drilling could be suspended to allow for specific sampling. At the end of the drilling, a long period of pumping was set before sampling until the stability of the conductivity log was reached (at least a week and up to 6 weeks).

Water samples were collected in three different ways (Table 2): (1) a global pumping (GP) with a submerged pump in the upper part of the water column (typically 150 m deep); (2) a selective pumping with a specifically designed diapo pump placed in front of the selected productive level with a pumping rate lower than the estimated water production rate; and (3) a 12- or 20-litre

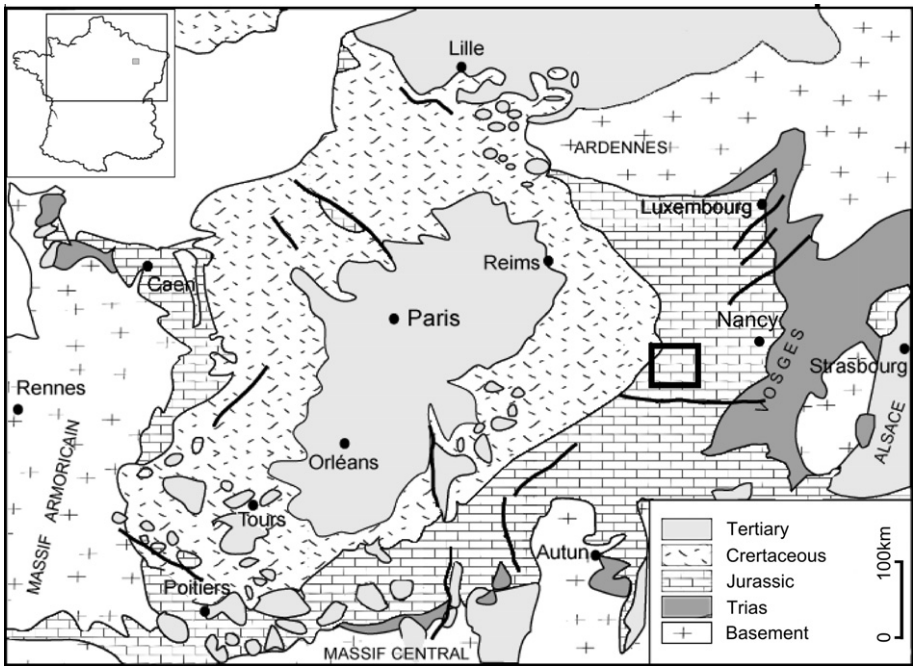

Fig. 1. Simplified map of the Paris Basin showing the location of the study area as a black square.

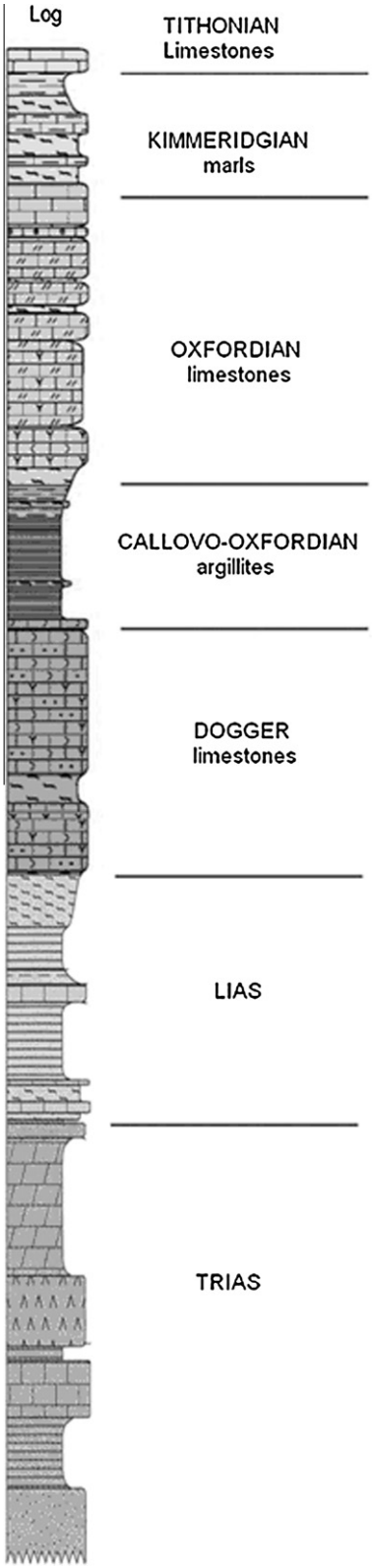

Fig. 2. Simplified stratigraphy of the study area showing main geological units. The depth varies from one borehole to another due to the locally varying thicknesses of the formations. For instance, the top of the COX is found at a depth of 400 m in borehole A and at a depth of 575 m in borehole F.

sampler (bottle) lowered to a selected depth, closed at the selected depth and brought back to the surface. A test was carried out to compare global pumping samples with the bottle samples, and the He concentrations agreed within 10%. This slight difference may be because the pumping method includes minor venues that are not sampled by the bottle.

On the surface, we used 3/8'' copper tubes directly connected by plastic tubing to the immerged pumps or the bottles as soon as they were brought back to the surface to maintain a continuous flow of fluids and so minimise any potential gas loss. After flushing the volume of the tubes (6 or 10 cc) several times, they were tightly closed at both ends by clamps. When collecting deep samples, gas loss can be a concern. Indeed, gas loss is a real issue for sites with large CO_2 or biogenic gas production, which can lead to supersaturation of the samples with respect to total gas solubility. However, there was no such gas supersaturation in our case. Therefore, even if the samples from our study are enriched in He, the total gas pressure is not markedly different from the equilibrium pressure, and there is thus no reason to suspect significant degassing while sampling. That no gas bubbles were observed during sampling confirms this conclusion.

In the lab, dissolved helium was extracted under vacuum into a glass bulb following our standard procedure (Jean-Baptiste et al., 1992). The yield of He transfer was measured as 99.95% with a one-sigma uncertainty of 1.2%. The glass bulbs were then connected to the high-vacuum stainless steel inlet line of a MAP-215-50 noble gas mass spectrometer. The resolution was better than 500, which allowed a good separation of ^{3}He and HD peaks (ion counting down to zero between the two peaks). The measurements were calibrated against an air standard. The one-sigma analytical uncertainties for helium concentrations and ^{3}He/^{4}He ratios are given in Table 2, including He transfer efficiency, calibration of the volumes of the introduction line, blanks uncertainty (extraction and measurement), statistical counting uncertainty and standard uncertainty.

3. Results

The results of the He measurements, given with one-sigma uncertainty, are summarised in Table 2. For 12 samples, two copper tubes were filled on-site, one after the other, and were analysed separately to check the reproducibility of our measurements (Fig. 4).

For the few water venues that could be discretely sampled, the helium results do not allow for a clear distinction between the different water venues, and no general trend is found with the sampling depth within each aquifer. Therefore, the scatter of He concentrations, which is larger than the reproducibility of the duplicates, probably reflects both the mixing of different water venues and the different sampling techniques (see Section 2).

3.1. Oxfordian aquifer

For sites A, C and F, the ^{4}He concentrations of the Oxfordian waters range from 3 to 6×10^{-10} mol/g (Fig. 5). These concentrations are more than two orders of magnitude greater than the He concentration in the air-saturated water (ASW at 10 °C: 2.1×10^{-12} mol/g, Weiss 1971). For site B, the water samples are even richer in He, with concentrations approximately twice as high as at sites A, C and F. For the Oxfordian groundwaters of these four boreholes, the isotopic ^{3}He/^{4}He ratios are highly radiogenic, with a mean value of 0.019 ± 0.002 Ra, which is close to a typical crustal production ratio (Ballentine and Burnard 2002).

The site E data display completely different characteristics, with ^{4}He concentrations 10 times lower and ^{3}He/^{4}He ratios between 0.18 and 0.33 Ra, showing an important contribution from atmosphere-derived He in these samples and a larger scatter than for the data from the other boreholes. This contribution will be further discussed in Section 4.1.1.

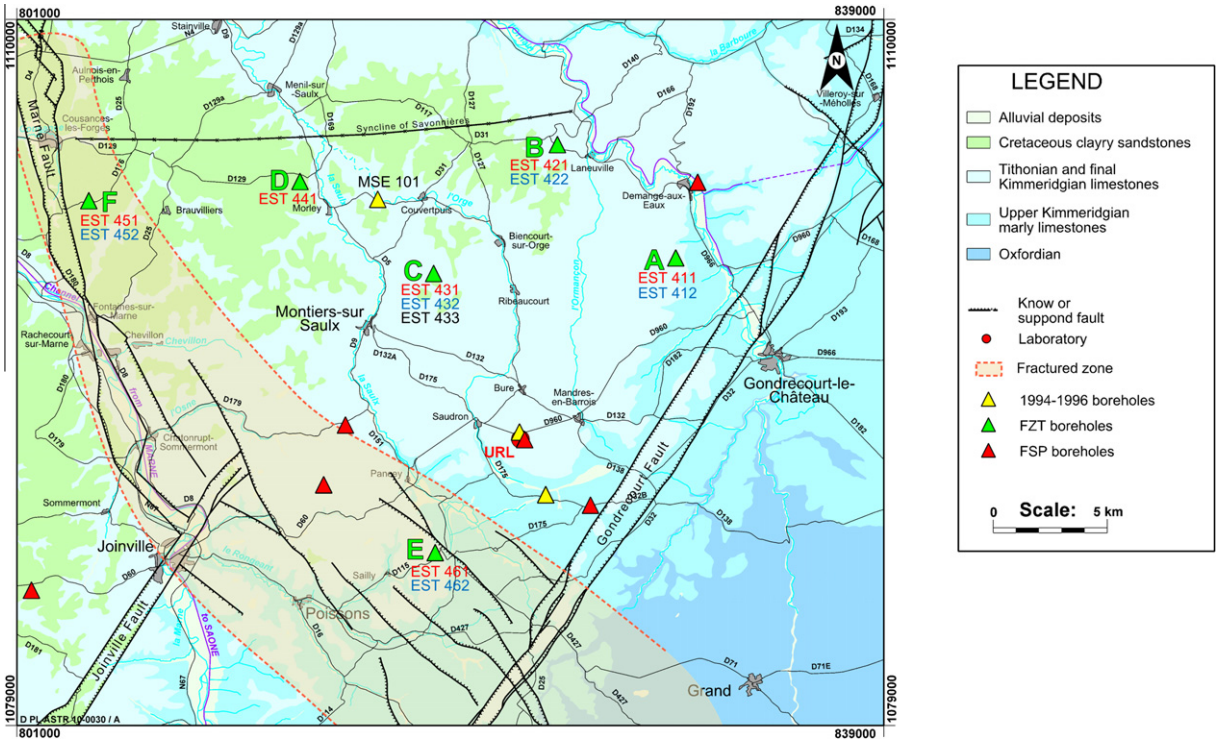

Fig. 3. Geological map of the study area with locations of the drillings.

Table 1
Main water venues and their respective contribution to the water column as determined from geochemical diagraphies and as reported by Andra (2009b).

Borehole	Depth interval of main water venues (m)	Contribution in (%)	Depth interval of main water venues (m)	Contribution in (%)
	Oxfordian free waters		Dogger free waters	
A-EST 411	159–174	28	630–633	51
A-EST 411	269–274	7	635–637	6
A-EST 411	281–292	14	641	12
A-EST 411	302–339	43	644–647	15
B-EST 422	297–304	67	713–718	19
B-EST 422	359–362	29	723–733	77
C-EST 431	297–301	11	698–703	93
C-EST 431	328–329	12	703–718	6
C-EST 431	412–414	12		
C-EST 431	438–440	15		
C-EST 431	505–507	50		
F-EST 451	431–433	65	775–785	81
F-EST 451	452–458	33	785–790	19
E-EST 461	165–178	76	559–564	99
E-EST 461	214–230	5		
E-EST 461	258–282	17		

3.2. Dogger aquifer

The Dogger groundwater samples show ^{4}He concentrations an order of magnitude greater than the Oxfordian samples (Fig. 6), ranging from 15 to 55 $\times$ 10^{-10} mol/g for sites A, C, E and F, and even 80–95 $\times$ 10^{-10} mol/g for site B. The helium isotopic ratios, in contrast, are exceptionally homogeneous, with a mean value of 0.0194 ± 0.0005 Ra. The two samples from site F, however, show a larger scatter compared with the samples from the other sites perhaps because this borehole is the only one that is artesian (EST 03298 was taken directly at the surface). In this case, the water venues are naturally moved upward in the borehole. Therefore, the sampling at 789 m with the diapo pump depth was not mixed with water from above, as it was likely in a non-artesian borehole. The lower He concentration observed in this sample is indeed consistent with He measurements in the limestone porewaters from drilling site C, which show a factor two decrease in the first 30 m of the Dogger (Waber and Vinsot, 2010).

3.3. Trias aquifer

Only one water venue encountered at a depth of 1880–1900 m could be sampled while drilling borehole C below the Dogger formation (the casing of the borehole prevented mixing with overlying groundwaters). This sample shows a He concentration of the same order of magnitude as the Dogger samples (twice as high as the Dogger values for the same drilling site), but the isotopic ratio is higher by a factor of two, at 0.04 Ra.

Table 2
He data for the Oxfordian, Dogger and Triassic groundwaters with one-sigma error bars. See text for the sampling methods. Concentrations are per gram of water. The samples display high He concentrations. To maintain the pressure in the mass spectrometer source within a range where the response of the mass spectrometer is linear, it was necessary to introduce only a fraction of the total volume of the sample. These steps induce additional uncertainties in the He concentration due to volume calibration, and they explain why the relative uncertainties differ from one sample to another.

Borehole	Sample reference	Long-term pumping	Sampling method	Sampling depth (m)	^{4}He (10^{-10} mol/g)	(^{3}He/^{4}He)/Ra
Oxfordian free waters						
A-EST411	EST 03306	✓	GP	150	3.84 ± 0.10	0.021 ± 0.001
A-EST411	EST 03310	✓	diapo	270	4.45 ± 0.20	0.016 ± 0.001
A-EST411	EST 03314	✓	diapo	347	6.03 ± 0.10	0.018 ± 0.001
B-EST 422	EST 02690		bottle	355	11.8 ± 0.44	0.018 ± 0.001
B-EST 421	EST 02930	✓	GP	150	14.1 ± 0.60	0.016 ± 0.001
B-EST 421	EST 02934	✓	bottle	290	14.1 ± 0.60	0.016 ± 0.001
C-EST431	EST 03052		diapo	395	4.02 ± 0.10	0.020 ± 0.001
C-EST431	EST 03043		diapo	500	5.62 ± 0.30	0.022 ± 0.003
C-EST431	EST 03323	✓	GP	150	4.62 ± 0.08	0.018 ± 0.001
C-EST431	EST 03331	✓	diapo	370	3.04 ± 0.05	0.022 ± 0.001
C-EST431	EST 03335	✓	diapo	490	3.62 ± 0.07	0.019 ± 0.001
F-EST451	EST 02864		GP	150	3.58 ± 0.08	0.021 ± 0.001
F-EST451	EST 02921		GP	150	3.74 ± 0.09	0.021 ± 0.001
F-EST451	EST 02925		bottle	450	3.62 ± 0.08	0.021 ± 0.001
F-EST451	EST 03290	✓	GP	150	3.65 ± 0.14	0.021 ± 0.001
F-EST451	EST 03294	✓	diapo	510	3.68 ± 0.09	0.023 ± 0.001
E-EST461	EST 02960		GP	150	0.239 ± 0.003	0.210 ± 0.004
E-EST461	EST 02964		bottle	200	0.182 ± 0.004	0.326 ± 0.011
E-EST461	EST 03261	✓	GP	150	0.165 ± 0.003	0.186 ± 0.005
E-EST461	EST 03265	✓	diapo	200	0.137 ± 0.006	0.227 ± 0.014
Dogger free waters						
A-EST 412	EST 03049	✓	GP	150	17.1 ± 0.5	0.019 ± 0.001
B-EST 422	EST 02837	✓	GP	150	83.5 ± 2.6	0.019 ± 0.001
B-EST 422	EST 02841	✓	bottle	150	93.9 ± 2.9	0.019 ± 0.001
B-EST 422	EST 02842	✓	bottle	715	80.6 ± 3.8	0.019 ± 0.001
C-EST 432	EST 03243		GP	150	27.4 ± 1.2	0.020 ± 0.001
C-EST 432	EST 03247		bottle	765	34.5 ± 1.3	0.020 ± 0.001
C-EST 432	EST03319	✓	GP	150	33.6 ± 0.4	0.019 ± 0.001
F-EST 452	EST03298F-10	✓	artesian	0	54.1 ± 2.3	0.019 ± 0.001
F-EST 452	EST03302F-10	✓	diapo	789	30.0 ± 1.3	0.020 ± 0.001
E-EST 462	EST03285F-10	✓	GP	150	21.7 ± 0.7	0.020 ± 0.001
Triassic free water						
C-EST 433	EST 03257		GP	150	67.0 ± 13.4	0.040 ± 0.002

4. Discussion

In this section, we will first discuss specific aspects of these data before interpreting them within the framework of a regional 2D simplified He transport model.

4.1. Data discussion

The mixing diagram in Fig. 7 shows that all the Dogger and Oxfordian (with the exception of site E) groundwaters are air-saturated waters that accumulated radiogenic crustal helium with an overall ^{3}He/^{4}He ratio of 0.02 Ra, reflecting both in-situ input and input from the underlying layers and basement. As noted above, sites A, C and F display rather similar helium characteristics, which differ significantly from those of site B and differ drastically from those of the Oxfordian drilling of site E. These two boreholes will, therefore, be specifically discussed below as well as the only groundwater sample collected in the Triassic formation.

4.1.1. The diffuse fractured zone

Technical difficulties were encountered during site E drilling, and an intrusion of young waters was suspected along the casing. However, Fig. 7 clearly shows that it is not only present-day air-saturated water that mixes with the Oxfordian water. The data plot is well above the mixing trend, thus indicating a tritiogenic ^{3}He component. The tritium measurements for these samples, which are within a range of 0.4–2.2 TU (Jean-Baptiste et al., 2010), confirm this point: only 3–6% of Oxfordian-type waters are needed to account for the ^{4}He concentrations measured at site E. This conclusion is supported by the chemistry of the major ions, such as the sulphate concentrations. These concentrations are <15 mg/L, which are close to those of the superficial water venues, while they are above 200 mg/L for the other boreholes (Andra, 2009b). A simple binary mixing between "post-bomb" water and the 3–6% Oxfordian-type water fails to reproduce both the "high" ^{3}He values and the "low" tritium values. Therefore, based on their helium and tritium concentrations, those waters are most likely at least a three-component mixture. Such mixing could, for example, explain the following data: (1) 3–6% Oxfordian-type water; (2) 2–8% superficial recent waters tagged with bomb tritium, which introduced approximately $2–5 \times 10^{-19}$ mol of tritiogenic ^{3}He; and (3) the remaining being "pre-bomb" water, which contains approximately 10^{-18} mol/g of natural tritiogenic ^{3}He from the above aquifer(s) (Kaufman and Libby, 1954).

For site F, which was drilled in the northern part of the same fractured zone, the He measurements provide no evidence of such a mixing with waters from more superficial aquifers (see below). We therefore think that the observed mixing in site E rather reflects an artefact due to the drilling operations (casing problem), which

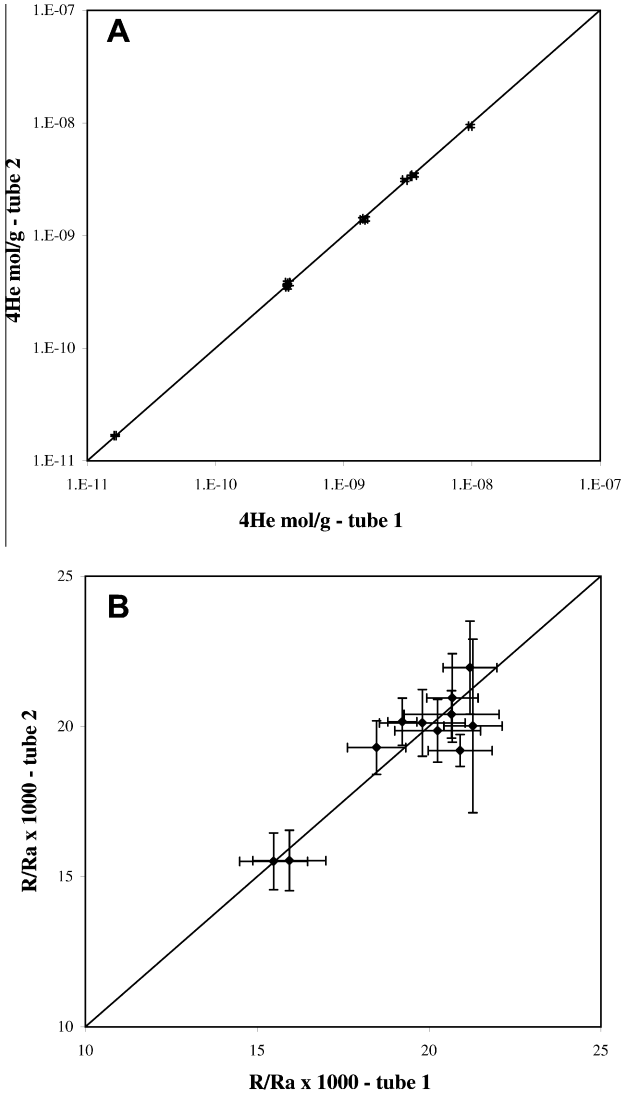

Fig. 4. Reproducibility of the He concentration (A) and isotopic ratio $^3He/^4He$ (B) measurements for duplicates (two copper tubes consecutively filled on site with the same water).

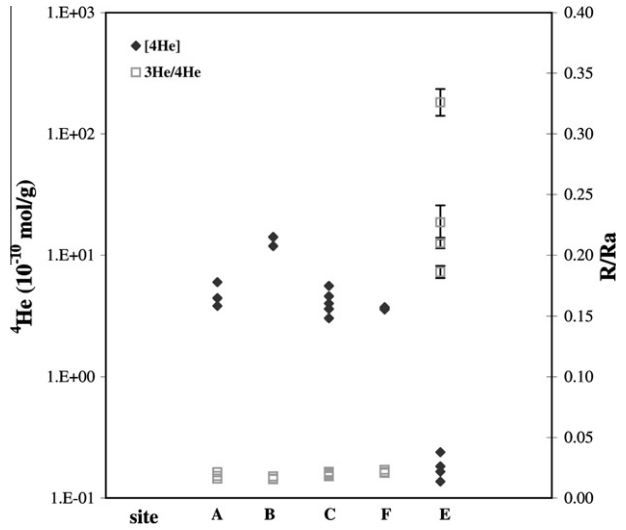

Fig. 5. He concentration and isotopic ratio of Oxfordian waters. Except for the isotopic ratio of site E, the error bars are within the symbol size.

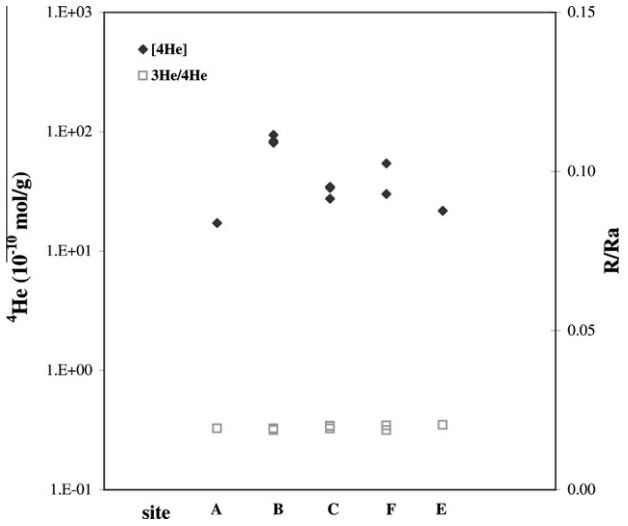

Fig. 6. He concentration and isotopic ratio for Dogger waters. Error bars are within the symbol size.

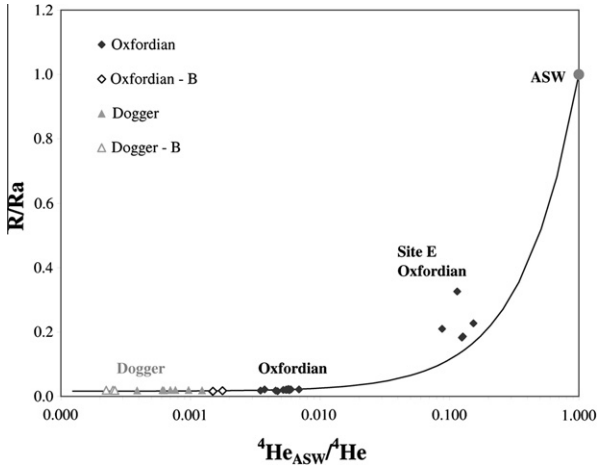

Fig. 7. Diagram of mixing between air-saturated water (ASW) and a crustal end-member with a ratio of 0.02 Ra.

artificially connected the aquifers, than a natural mixing of groundwaters across different sedimentary units through diffuse fractures.

Note, however, that for site F, based on the He data only, it is not possible to discard completely any natural intrusion of a small amount of above Tithonian waters, as the composition of the Tithonian aquifer in this part of the site might shift away from the ASW characteristics. Dewonck (2000), for example, identified a second group of Tithonian waters sampled in Auzécourt or Laheycourt approximately 40 km north of site F, with He isotopic ratios of approximately 0.07 Ra and He concentrations within a range of 10^{-10} mol/g. To conclude, it would be necessary to study the Tithonian waters from borehole F to investigate the lateral characterisation of Tithonian waters.

4.1.2. Borehole B singularity

Site B, which was drilled in the northernmost part of the area investigated during this campaign, shows He concentrations approximately two to three times higher than those in the groundwaters from the other sites, both in the Oxfordian and the Dogger formations. Marty et al. (2003) measured noble gases in a groundwater sample from the Dogger collected in a nearby borehole, designated MSE 101 (Fig. 3). These authors determined a He

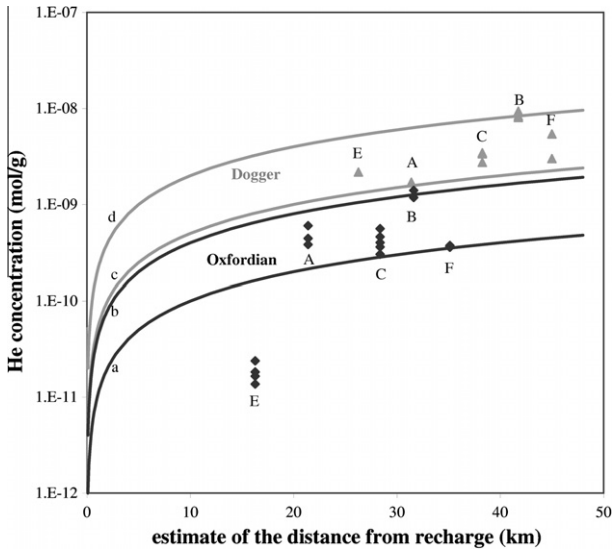

Fig. 8. Helium concentrations in the Oxfordian (black diamonds) and Dogger (grey triangles) aquifers as a function of the estimated distance to the recharge area. Solid lines a–d represent constant helium accumulations of, respectively, 0.1, 0.4, 0.5 and 2×10^{-10} mol/g of water/km.

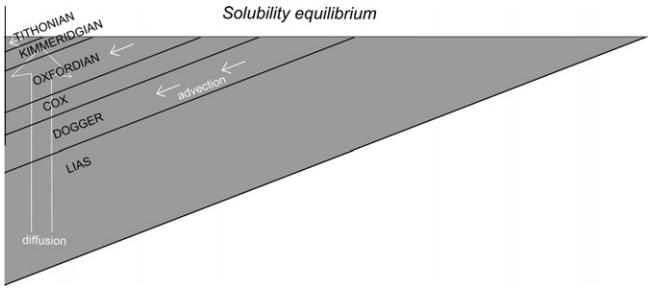

Fig. 9. Simplified diagram of the geometry of the 2D model described in Section 4.2.

concentration of 73×10^{-10} mol/g with an isotopic ratio of 0.023 Ra. These values are in good agreement with ours for the Dogger groundwaters of borehole B (Table 2).

From the localisation of the recharge area for both aquifers, as determined by Andra (piezometric maps in Andra 2005), we can determine the order of magnitude of the He accumulation gradient (visual fitting from data in Fig. 8) as follows: between 0.1 and 0.4×10^{-10} mol/g/km for the Oxfordian waters and between 0.5 and 2×10^{-10} mol/g/km for the Dogger waters. This graph clearly shows that the He accumulation gradient is higher at site B for both aquifer formations.

Two hypotheses, which are not mutually exclusive, can be considered to explain these data: (1) the circulation of water in this part of the studied area is slow, allowing He to accumulate (e.g., in an area away from the main flow lines, where waters are more stagnant); or (2) the helium flux from below is locally high (as a matter of fact, it is highly unlikely that only a change in the uranium and/or thorium composition of the aquifer host rock can account for these greater He values in site B).

These two hypotheses are further investigated in Section 4.2 based on a simplified 2D model of the diffusive and advective helium transport across the sedimentary pile.

4.1.3. Glimpse of the Trias groundwaters

Various authors have analysed noble gases in the Triassic waters from the centre of the Paris Basin (Castro et al., 1998a; Pinti and Marty, 1998) and from wells close to the eastern recharge area, which is a few tens of kilometres east of site C (Marty et al., 2003). These latter wells show relatively high $^3He/^4He$ ratios, from 0.25 up to 0.64 Ra. Marty et al. (2003) explain these data by the input of a mantle-derived ^3He component due to the proximity of the Rhine graben.

In this study, only one water sample from the Trias formation was recovered ($^3He/^4He = 0.040 \pm 0.002$ Ra), limiting the scope of any interpretation. However, it is interesting that, even from within a short distance (site C is only 40–50 km west of the eastern samples analysed by Marty et al., 2003), the "mantle-derived signature" of the Triassic waters is no longer obvious. We consider that the most likely explanation is a dilution of the mantle-derived He by a radiogenic component. This process implies that the velocities (1–7 m/yr estimated from ^{14}C ages by Marty et al., 2003) quickly slow down as the waters flow westward to allow for the accumulation of radiogenic He. Such a process is in agreement with the fact that, east of Nancy, the Triassic waters rapidly become too mineralised to be exploited for drinking water. Baudricourt and La Neuville are the two sampling points from the Marty et al. (2003) study that are closest to site C, and the reported He concentrations are 1.2 and 1.6×10^{-9} mol/g, respectively (with $^3He/^4He$ ratios of 0.32 and 0.30 Ra, respectively). If we consider that He with a ratio of 0.02 Ra is added to reach the 6.7×10^{-9} mol/g measured in site C, then the ratios obtained are within the range 0.05–0.07 Ra, the same order of magnitude as our site C measurement. This result implies an accumulation of He between 1.0 and 1.2 mol/g/km, which is quite realistic as it is the same order of magnitude as our values for the Dogger aquifer.

4.2. Helium transport model

^4He transport is simulated using a 2D model with a simplified geometry (Fig. 9). The main characteristics of the modelled stratigraphic units are summarised in Table 3. Because the helium flux at the base of the domain is unknown, we adopt as a boundary condition the helium concentration in the porewater measured at the base of the Lias in site C, which is $[^4He] = 5 \times 10^{-4}$ ccSTP/g (Waber and Vinsot, 2010). At the surface, the He concentration is taken at the solubility equilibrium of $T = 10$ °C. We consider vertical helium diffusion through porewater in all stratigraphic units and additional advective horizontal transport in the aquifers through the portion of the total porosity that is thought to be accessible

Table 3
Main characteristics of the 2D helium transport model. ^4He production is estimated from U and Th data available in Andra (2005) and integrated over the whole thickness of each stratigraphic layer.

Main stratigraphic units	Depth (m)	Distance to recharge	Total porosity (ω_t)	Free water porosity (ω_a)	D_e (m^2/s) case a	D_e (m^2/s) case b	Helium production ($mol/m^2/yr$)
Tithonian Limestone	0–100	10 km	0.1	0.1	2×10^{-11}	2×10^{-10}	2.35×10^{-9}
Kimmeridgian marls	100–220	–	0.15	0	2×10^{-11}	2×10^{-11}	6.36×10^{-9}
Oxfordian Limestone	220–480	30 km	See Fig. 10	See Fig. 10	2×10^{-11}	2×10^{-10}	6.69×10^{-9}
Cox argillites	480–620	–	0.18	0	2×10^{-11}	2×10^{-11}	7.15×10^{-9}
Dogger Limestone	620–850	40 km	See Fig. 10	See Fig. 10	2×10^{-11}	2×10^{-10}	2.39×10^{-9}
Lias argillites	850–1150	–	0.15	0	2×10^{-11}	2×10^{-11}	1.59×10^{-8}

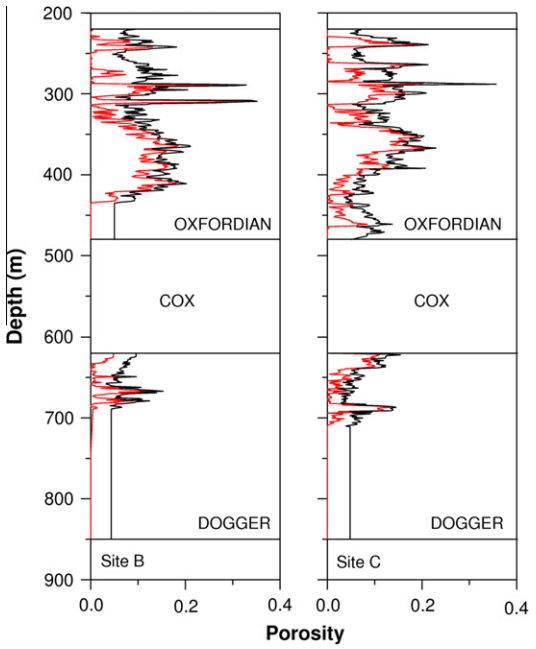

Fig. 10. Total porosity profile in black (considered for diffusion processes) and free water porosity profile in red (considered for advective transport) for the Oxfordian and Dogger limestone formations, obtained in-situ by nuclear magnetic resonance in boreholes B and C (Andra, 2009a). A composite depth scale of boreholes B and C is proposed to make comparisons easier. The low porosity values in the limestones are due to porosity cementation through time (Brigaud et al, 2009) and are a key factor in understanding such "old" groundwater ages obtained by the model at this site.

to advection (i.e., the free water porosity in Fig. 10). The 2D helium distribution is described by the classic diffusive-advective equation with all layers considered to be isotropic:

$$\omega_t \partial C/\partial t = D_e \partial C^2/\partial z^2 + \omega_a v \partial C/\partial x + P_{\mathrm{He}} \rho_r (1 - \omega_t)$$

where C is the helium concentration in the porewater, D_e is the effective helium diffusion coefficient, v is the advection velocity, ω_t is the total porosity, ω_a is the porosity accessible to advection, P_{He} is the ^{4}He production rate per mass unit of rock due to U–Th decay and ρ_r is the rock density. The helium release efficiency is assumed to be ~1, as suggested by the work of Dewonck (2000) in the same area and, more generally, by helium data in similar geological settings, which show that the rocks and minerals have almost completely lost radiogenic in-situ-produced helium (Tolstikhin et al., 1996). For D_e, we test two hypotheses: (a) a "low" diffusivity case, where for all stratigraphic units we adopt a value of 2×10^{-11} m^2/s, as determined from tritium diffusion experiments (Descostes et al., 2008) and helium diffusion coefficients in free water (Jähne et al., 1987) (this value is close to the apparent diffusion coefficient derived from the He profile in a similar formation, the Opalinus clay of Mont Terri, at 3.5×10^{-11} m^2/s; see Rübel et al., 2002); and (b) a "high" diffusivity case, where for the aquifers, we adopt a diffusion coefficient 10 times higher (to take into account, e.g., the effect of dispersion).

The diffusion-advection equation is solved numerically with vertical and horizontal steps, being $\Delta z = 1$ m and $\Delta x = 5$ km, respectively. A steady state is reached in approximately 20 Myr. Fig. 11a and b shows the simulated He profiles for sites B and C, which were selected because they represent the two extremes in He concentrations recorded in the COX porewaters (Smith, 2010).

For site C, the residence times of the Dogger and Oxfordian waters that produce the best visual fit to the data are 0.6 and 0.5 Myr, respectively, in case a, and 0.5 and 0.3 Myr, respectively, in case b. We must remember that these values are only indicative due to the oversimplified nature of the model. The two sets of residence times are in the same range, but the Oxfordian age of case b is more consistent with ^{36}Cl/Cl ratios measured in boreholes from a previous drilling campaign in the same area (Lavastre et al., 2010), which show values above the secular equilibrium for the Oxfordian samples.

For site B, the exact He concentration at the bottom of the domain is not precisely known (contrary to site C). Therefore, as stated above (Section 4.2), the higher helium concentrations could, a priori, reflect older ages of the waters or a larger He supply from below. Our simulations with the same boundary condition as for site C give Dogger and Oxfordian ages of 1.5 and 1.4 Myr, respectively, for case a and 1.5 and 0.8 Myr, respectively, for case b. Older

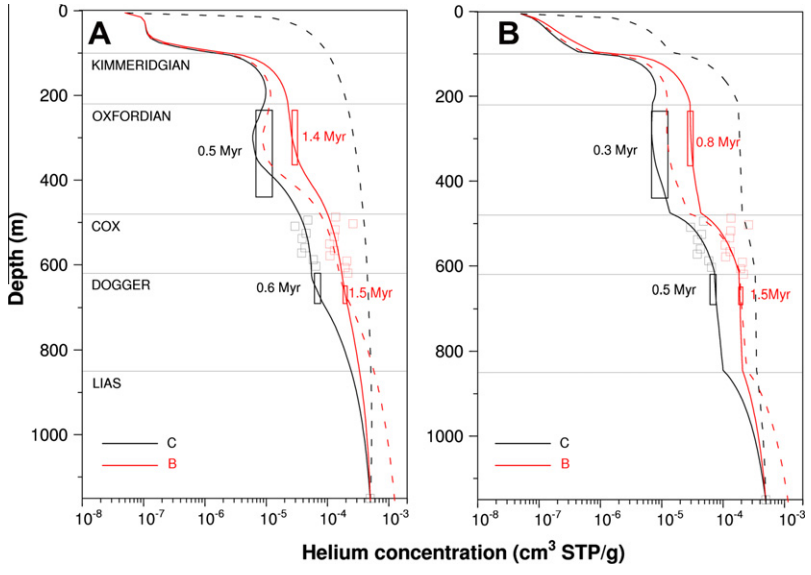

Fig. 11. Helium concentration data are represented as squares in the COX (Smith, 2010) and as rectangles in adjacent groundwaters over the depth range corresponding to water inflows (this work). Simulated helium profiles are drawn for (a) the "low" diffusion case and (b) the "high" diffusion case (see text). Site B is in red and site C in black. The helium concentration at the base of the Lias (site C) is from Waber and Vinsot (2010). The solid curves are the simulated helium profiles with the Dogger and Oxfordian water residence times tuned to fit the data (the corresponding residence times are indicated in the figure). The dashed red curves correspond to site B with the same groundwater residence times as for site C, but with a higher He boundary concentration at the base of the Lias, which is tuned to fit the Dogger data. The dashed black curves correspond to diffusion only.

Table 4
Helium fluxes computed at the base of each stratigraphic unit by the 2D advection-diffusion model.

	Entering vertical fluxes (mol/m^2/an)	
	Site B	Site C
	Case a	*Case a*
Lias	7.6E−09	1.6E−08
Dogger	2.3E−08	3.2E−08
Cox	1.1E−08	4.7E−10
Oxfordian	1.8E−08	7.7E−09
Kimmeridgian	1.5E−09	−1.5E−09
Tithonian	7.8E−09	4.9E−09
	Case b	*Case b*
Lias	1.9E−08	2.8E−08
Dogger	3.5E−08	4.4E−08
Cox	2.4E−08	8.0E−09
Oxfordian	3.1E−08	1.5E−08
Kimmeridgian	3.1E−09	−1.9E−09
Tithonian	9.5E−09	4.5E−09

ages for the Dogger aquifer are also suggested by ^{36}Cl/Cl values close to the secular equilibrium in Lavastre et al. (2010) for nearby boreholes. In Fig. 11a and b, the red dashed line shows the helium profile obtained for site B when setting the same water ages as in site C and raising the He concentration at the bottom of the domain. Whereas the measured helium concentrations in the Dogger could be attained by raising He concentration at the bottom boundary, the model shows that this is insufficient to obtain high He concentrations in the Oxfordian without raising the age of the water. Therefore, the model results are more in favour of the older ages hypothesis, thus suggesting that both the Dogger and Oxfordian aquifers are more stagnant in this part of the studied area.

Previous estimates of Dogger groundwater residence times cover a wide range, from 10^3 years (Aubertin et al., 1987) or 10^5 years (Wei et al., 1990) to 4 Myr, as estimated by Marty et al. (1993), who argued that relatively rapid hydrologic flow velocities are inconsistent with the water geochemistry. In a study including He and Ar isotopes, Castro et al. (1998a,1998b) suggested a much younger age of approximately 100 ka. However, these estimates are not straightforwardly comparable to ours because these are large-scale studies that are focused on the centre of the basin (Paris region) and, therefore, do not reflect regional specificities. Dewonck (2000) studied a basin-scale groundwater flow model with a refined description of the area around the Underground Research Laboratory (URL). This study presented a groundwater residence time of approximately 1 Ma at MSE 101 (Fig. 3), which is consistent with our estimates.

The modelled helium fluxes at the interfaces of the stratigraphic units for both diffusion cases (a) and (b) are shown in Table 4 for sites B and C. The He flux at the bottom of the domain is within a range of 0.76–2.84 $\times$ 10^{-8} mol/m^2/yr for the various cases investigated. This value is much less than the global mean crustal flux of 1.5 $\times$ 10^{-6} mol/m^2/yr (O'Nions and Oxburgh, 1983), thus pointing to the role of the lower Trias aquifer in diverting this crustal flux. It is also noticeable in the model outputs of Table 4 that a large fraction of the He flux entering the domain and of the He production in the different geological layers is flushed by horizontal advection in the Dogger and Oxfordian aquifers.

5. Conclusions

The aim of this study was to investigate He concentrations and isotopic ratios in the aquifers sandwiching the clay-rich Callovo-Oxfordian across the studied zone defined by Andra, which is close to the Underground Research Laboratory. Our main observations and conclusions are as follows:

- He concentrations are two orders of magnitude higher than air-saturated water in the Oxfordian and approximately 10 times higher in the Dogger. All Dogger and Oxfordian groundwaters (with the exception of site E) are air-saturated waters that have accumulated radiogenic helium with a ^{3}He/^{4}He ratio of 0.02 Ra.
- The Oxfordian part of borehole E displays anomalous characteristics. Based on helium isotopes and tritium, these waters are a three-component mixture of the following: (1) 3–6% Oxfordian-type water; (2) 2–8% recent waters tagged with bomb tritium; and (3) the remaining "pre-bomb" water. The observed mixing is most probably an artefact from a casing problem encountered while drilling and artificially connecting the aquifers.
- Only one sample was recovered from the Trias. The He concentration of this sample is of the same order of magnitude as those measured in the Dogger, with a higher isotopic ratio of 0.04 Ra. However, this ratio is much lower than those (0.25–0.64 Ra) measured by Marty et al. (2003) a few tens of kilometres eastwards, upstream of the Dogger recharge outcrops. We consider that the most likely explanation is a significant slow-down of the Triassic water circulation, inducing radiogenic He accumulation and a subsequent dilution of the mantellic ^{3}He component identified by Marty et al. (2003). A rough calculation of the required addition of radiogenic He shows that the orders of magnitude involved by this hypothesis are consistent with the accumulation rates estimated for the above aquifers.
- Helium data show that the transposition zone is not horizontally homogeneous: the He concentrations in the Oxfordian and Dogger groundwaters are higher in the northern part of the investigated area (borehole B). This result echoes the results of He concentrations in the COX porewaters, which are also higher in borehole B (Smith, 2010). A simplified 2D model of the He transport allows us to conclude that an older water age is a more likely explanation than a higher He input from below, at least for the Oxfordian. The residence time estimates from this model are within a range of 0.5–0.6 Myr and 0.3–0.5 Myr for the Dogger and Oxfordian, respectively, at site C and 1.5 Myr (Dogger) and 0.8–1.4 Myr (Oxfordian) for the northern borehole B. This difference in residence times between sites B and C is consistent with the chemistry results of Rebeix (2010), which show much more mineralised water at site B than elsewhere. This result confirms earlier results on COX porewater given by Gaucher et al. (2006), who showed a decrease of Na and Cl concentrations along a NE-SW axis across the study area.

These residence times are only indicative due to the simplicity of the model and the coarse hypotheses made. A ^{36}Cl/Cl analysis of these very boreholes and an interpretation of the δ^{37}Cl profiles (as in Lavastre et al., 2005) will provide further clues to the water residence times in the aquifers (Rebeix, 2010). A global 3D hydrological model of the area will be necessary to understand the heterogeneity of the transposition zone and, in particular, the reasons for the more stagnant waters around site B.

Acknowledgements

This study was funded by Andra via the GNR FORPRO program (TDC and TAPSS-2000 projects). We are grateful to all organisations and individuals, especially R. Rebeix, who assisted with the fluid samplings. We thank Ratan Mohapatra and an anonymous reviewer for their comments, which helped improve the manuscript.

References

Andra, 2005. Dossier 2005 Référentiel du Site Meuse/Haute-Marne Tome 1. C.RP.ADS.04.0022.

Andra, 2009a. Mise en Relation des Données Géochimiques Avec les Données Hydrogéologiques et Géochimiques Sur les Encaissants. Note Technique Centre de Meuse/Haute-Marne D.NT.ASMG.09.0063.

Andra, 2009b. Résultats Géochimiques Sur les Fluides des Encaissants et du Trias Prélevés Dans les Forages de la Campagne FZT. Note Technique Laboratoire de Recherche Souterrain Meuse/Haute-Marne D.NT.ALS.09.0541.

Aubertin, G., Cordier, E., Doillon, F., Fabris, H., Gable, R., Gaillard, B., Ledoux, E., de Marsily, G., Menjoz, A., 1987. Détermination expérimentale de la vitesse d'écoulement de la nappe géothermique du Dogger en région parisienne. Bull. Soc. Geol. Fr. 1, 991–1000.

Ballentine, C.J., Burnard, P., 2002. Production release and transport of noble gases in the continental crust. In: Porcelli, D., Ballentine, C.J., Wieler, R. (Eds.), Noble Gases in Geochemistry and Cosmochemistry. Rev. Mineral. Geochem., vol. 47, pp. 481–538.

Ballentine, C.J., Burgess, R., Marty, B., 2002. Tracing fluid origin, transport and interaction in the crust. In: Porcelli, D., Ballentine, C.J., Wieler, R. (Eds.), Noble Gases in Geochemistry and Cosmochemistry. Rev. Mineral. Geochem., vol. 47, pp. 539–614.

Brigaud, B., Durlet, C., Deconinck, J.-F., Vincent, B., Thierry, J., Trouiller, A., 2009. The origin and timing of multiphase cementation in carbonates: impact of regional scale geodynamic events on the Middle Jurassic Limestones diagenesis (Paris Basin, France). Sediment. Geol. 22, 161–180.

Buschaert, S., Giannesini, S., Lavastre, V., Benedetti, L., Gaucher, E., Lacroix, M., Lavielle, B., Michelot, J.-L., France-Lanord, C., Bourles, D., Lancelot, J., Benabderrahmane, H., Dewonck, S., Vinsot, A., 2007. The contribution of water geochemistry to the understanding of the regional hydrogeological system. Mem. Soc. Geol. Fr. 178, 91–114.

Castro, M.C., Jambon, A., de Marsily, G., Schlosser, P., 1998a. Noble gases as natural tracers of water circulation in the Paris Basin 1 – measurements and discussion of their origin and mechanisms of vertical transport in the basin. Water Resour. Res. 34, 2443–2466.

Castro, M.C., Goblet, P., Ledoux, E., Violette, S., de Marsily, G., 1998b. Noble gases as natural tracers of water circulation in the Paris Basin 2 – calibration of a groundwater flow model using noble gas isotope data. Water Resour. Res. 34, 2467–2483.

Clarke, W.B., Jenkins, W.J., Top, Z., 1976. Determination of tritium by mass spectrometric measurements of ^{3}He. Int. J. Appl. Radiat. Isot. 27, 515–522.

Descostes, M., Blin, V., Bazer-Bachi, F., Meier, P., Grenut, B., Radwan, J., Schlegel, M.L., Buschaert, S., Coelho, D., Tevissen, E., 2008. Diffusion of anionic species in Callovo-Oxfordian argillites and Oxfordian limestones (Meuse/Haute-Marne, France). Appl. Geochem. 23, 655–677.

Dewonck, S., 2000. Géochimie Isotopique des Gaz Rares Dans les Roches Sédimentaires et les Eaux Souterraines de l'est du Bassin Parisien. PhD Institut National Polytechnique de Lorraine, France.

Gaucher, E.C., Blanc, P., Bardot, F., Braibant, G., Buschaert, S., Crouzet, C., Gautier, A., Girard, J.-P., Jacquot, E., Lassin, A., Negrel, G., Tournassat, C., Vinsot, A., Altamnn, S., 2006. Modelling the porewater chemistry of the Callovo-Oxfordian formation at a regional scale. CR Geosci. 338, 917–930.

Jähne, B., Heinz, G., Dietrich, W., 1987. Measurement of the diffusion coefficients of sparingly soluble gases in water. J. Geophys. Res. 92, 10767–10776.

Jean-Baptiste, P., Mantisi, F., Dapoigny, A., Stievenard, M., 1992. Design and performance of a mass spectrometric facility for measuring helium isotopes in natural waters and for low level tritium determination by the ^{3}He ingrowth method. Int. J. Radiat. Appl. Instrum. (Part A) 43 (7), 881–891.

Jean-Baptiste, P., Fourré, E., Dapoigny, A., Michelot, J.-L., Massault, M., Noret, A., Rebeix, R., Le Gal La Salle, C., Aquilina, L., Labasque, T., Vinsot, A., 2010. Difficulty in assessing low ^{3}H, ^{14}C and ^{36}Cl concentrations in old groundwaters and its implication for groundwater dating – Andra 2007/2008 drilling program (Meuse/Haute Marne). In: 4th Int. Meeting, Clays in Natural and Engineered Barriers for Radioactive Waste Confinement (Abstract vol.).

Kaufman, S., Libby, W.F., 1954. The natural distribution of tritium. Phys. Rev. 93, 1337–1344.

Kipfer, R., Aeschbach-Hertig, W, Peeters, F., Stute, M., 2002. Noble gases in lakes and ground waters. In: Porcelli, D., Ballentine, C.J., Wieler, R. (Eds.), Noble Gases in Geochemistry and Cosmochemistry. Rev. Mineral. Geochem., vol. 47, pp. 615–700.

Lavastre, V., Jendrzejewski, N., Agrinier, P., Javoy, M., Evrard, M., 2005. Chlorine transfer out a very low permeability clay sequence (Paris Basin, France): ^{35}Cl and ^{37}Cl evidence. Geochem. Cosmochim. Acta 68, 4949–4961.

Lavastre, V., Le Gal La Salle, C., Michelot, J-L., Giannesini, S., Benedetti, L., Lancelot, J., Lavielle, B., Massault, M., Thomas, B., Gilabert, E., Bourlès, D., Clauer, N., Agrinier, P., 2010. Establishing constraints on groundwater ages with ^{36}Cl, ^{14}C, ^{3}H, and noble gases: a case study in the eastern Paris basin, France. Appl. Geochem. 25, 123–142.

Linard, Y., Vinsot, A., Vincent, B., Delay, J., Scholz, E., Lundy, M., Garry, B., Wechner, S., de La Vaissière, R., Cruchaudet, M., Dewonck, S., Vigneron, C., 2010. Water Flow in the Oxfordian and Dogger Limestone Around the Meuse/Haute-Marne Underground Research Laboratory, this volume.

Marty, B., Torgersen, T., Meynier, V., O'Nions, R., de Marsily, G., 1993. Helium isotopes fluxes and groundwater ages in the Dogger aquifer, Paris Basin. Water Resour. Res. 29, 1025–1035.

Marty, B., Dewonck, S., France-Lanord, C., 2003. Geochemical evidence for efficient isolation over geological timeframes. Nature 425, 55–58.

Matray, J.M., Lambert, M., Fontes, J.C., 1994. Stable isotope conservation and origin of saline waters from the Middle Jurassic aquifer of the Paris Basin, France. Appl. Geochem. 9, 297–309.

Mégnien, C., 1980. Synthèse géologique du Bassin de Paris. Mémoire du BRGM 101, 1–466.

O'Nions, R.K., Oxburgh, E.R., 1983. Helium-3 anomalies and crust-mantle interaction in Italy. Geochim. Cosmochica Acta 49, 2505–2513.

Pinti, D., Marty, B., 1998. The origin of helium in deep sedimentary aquifers and the problem of dating very old groundwaters. In: Parnell, J. (Ed.), Dating and Duration of Fluid Flow and Fluid-rock Interaction, Geological Society, vol. 144. Special Publications, London, pp. 53–68.

Rebeix, R., 2010. Datation, Traçage de L'origine et Traçage des Transferts des Eaux et des Solutés au Sein D'aquifères Profonds. PhD Paul Cezanne University, France.

Rübel, A.P., Sonntag, C., Lippmann, J., Pearson, F.J., Gautschi, A., 2002. Solute transport in formation of very low permeability: profiles of stable isotope and dissolved noble gas contents of pore water in the Opalinus Clay, Mont Terri, Switzerland. Geochim. Cosmochica Acta 66, 1311–1321.

Smith, T., 2010. Transfert Vertical des Gaz Rares à l'échelle des Différentes Formations de la Zone de Transposition du Site de Meuse/Haute-Marne et à L'échelle des Eaux Porales de L'argilite et du Callovo-Oxfordien. PhD Bordeaux I University, France.

Tolstikhin, I., Lehmann, B.E., Loosli, H.H., Gautschi, A., 1996. Helium and argon isotopes in rocks, minerals, and related groundwaters: a case study in northern Switzerland. Geochim. Cosmochimica Acta 60, 1497–1514.

Waber, H.N., Vinsot, A., 2010. Unraveling solute fluxes across the aquitard-aquifer sequence in the eastern Paris Basin; pore water tracer data from borehole EST 433. In: 4th Int. Meeting, Clays in Natural and Engineered Barriers for Radioactive Waste Confinement (Abstract vol.).

Wei, H., Ledoux, E., de Marsily, G., 1990. Regional modelling of groundwater flow and salt and environmental tracers transport in deep aquifers in the Paris basin. J. Hydrol. 120, 341–358.

Weiss, R., 1971. Solubility of helium and neon in water and seawater. J. Chem. Eng. data 16 (2), 235–241.